# Finite-size effects of hysteretic dynamics in multilayer graphene on a ferroelectric

Anna N. Morozovska, Anastasiia S. Pusenkova, Oleksandr V. Varenyk, Sergei V. Kalinin, Eugene A. Eliseev, and Maxym V. Strikha

Phys. Rev. B **91**, 235312 — Published 11 June 2015

DOI: 10.1103/PhysRevB.91.235312

# Finite size effects on hysteretic dynamics in multi-layer graphene on ferroelectric

**Anna N. Morozovska[1], Anastasiia S. Pusenkova[2], Oleksandr V. Varenyk[1], Sergei V. Kalinin[3], Eugene A. Eliseev[4], and Maxym V. Strikha[5*]**

[1]*Institute of Physics, National Academy of Sciences of Ukraine, Kyiv, Ukraine*

[2]*Taras Shevchenko Kyiv National University, Physics Faculty, Kyiv, Ukraine*

[3] *The Center for Nanophase Materials Sciences and Materials Science and Technology Division, Oak Ridge National Laboratory, Oak Ridge, TN 37831*

[4]*Institute for Problems of Material Sciences, National Academy of Sciences of Ukraine, Kyiv, Ukraine*

[5] *V.E. Lashkarev Institute of Semiconductor Physics, National Academy of Sciences of Ukraine, Kyiv, Ukraine*

## Abstract

The origin and influence of finite size effects on the nonlinear dynamics of space charge stored by multi-layer graphene on ferroelectric and resistivity of graphene channel were analyzed. Here, we develop a self-consistent approach combining the solution of electrostatic problems with the nonlinear Landau-Khalatnikov equations for ferroelectric. The size-dependent behaviors are governed by the relations between the thicknesses of multi-layer graphene, ferroelectric film and the dielectric layer. The appearance of charge and electro-resistance hysteresis loops and their versatility stem from the interplay of polarization reversal dynamics and its incomplete screening in an alternating electric field. These features are mostly determined by the dielectric layer thickness. The derived analytical expressions for electric fields and space charge density distribution in a multi-layer system enable knowledge-driven design of graphene-on-ferroelectric heterostructures with advanced performances. We further investigate the effects of spatially non-uniform ferroelectric domain structures on the graphene layers conductivity and predict its dramatic increase under the transition from multi- to single- domain state in ferroelectric. This intriguing effect can open new possibilities for the graphene-based sensors and explore the physical mechanisms underlying in the operation of graphene field effect transistor with ferroelectric gating.

[*] Corresponding author e-mail: maksym_strikha@hotmail.com

## 1. Introduction

The seminal works by Geim and Novoselov [1, 2, 3] became the harbinger of the new area of graphene physics at the junction between condensed matter and surface physics and physical chemistry. In the initial wave of graphene research, the attention of scientific community has been primarily focussed on the properties of graphene per se. However, it has been rapidly realized that many unique functionalities of graphene are strongly affected by interaction with substrate, gates, contacts, thermostat, and surface and interface adsorbates [4, 5].

Particularly of interest are the studies of graphene on the substrates with high permittivity, since these allow to achieve a higher carrier concentration for the same gate voltages [5, 6, 7]. In particular, using ferroelectrics instead of traditional high-k substrates offers dual advantage of high dielectric constant and non-volatile memory effects via polarization switching [8, 9, 10, 11, 12, 13, 14, 15]. Here, the charge carriers in a graphene screen the depolarization electric field induced by discontinuity of spontaneous polarization at the ferroelectric surface [16, 17, 18]], allowing for dynamic control of carrier concentration in graphene. The first study focused on graphene-on-ferroelectric device appeared in 2009 [8], and the number of such works have permanently increased, and several reviews have already been published (see e.g. [19, 20, 21]).

Notably, hysteretic ferroelectric gating and symmetrical bit writing in GFeFETs with an electro-resistance change of over 500% and a reproducible, nonvolatile switching have been demonstrated [10]. However, a comprehensive understanding of the nonlinear, hysteretic ferroelectric gating in GFeFETS is still absent [10]. This motivates us to develop the continuum media theory of the size effects influenced on the storied charge and electro-resistance nonlinear hysteretic dynamics in the multi-layer graphene on ferroelectric.

Below we present the modified continuum media approach, which combines the solution of electrostatic problem with the nonlinear Landau-Khalatnikov equation in a self-consistent way in order to describe analytically the nonlinear dynamics of the ferroelectric polarization reversal. We note that the continuum media approach is non-applicable to a mono-layer graphene and partially applicable to ultra-thin graphite layers. However the approach has the unique advantage to yield universal analytical expressions in terms of specific material parameters. As such, it can be directly matched to experiment. Here, we consider dynamic hysteretic effects in graphene layers of finite thickness extending thermodynamic studies [17], obtain analytical expressions for electric fields and space charge density distribution in a multi-layer system and establish the impact of buffer dielectric layer between graphene and ferroelectric surface in multidomain state. The analytical results allow a comprehensive

understanding of the physical process, as well as to predict and to analyze multi-scale size effects in the system, which opens an effective way to control and optimize its nonlinear and hysteretic properties.

## 2. Problem statement

Geometry of the considered GFeFET with two gates (similar geometry was used in [8, 10]) is shown in the **Figure 1.** Multi-layered graphene (MLG) of thickness $d$ has a background permittivity $\varepsilon_G$. Ultra-thin dielectric layer has thickness $h$ and dielectric permittivity $\varepsilon_d$. We note that this imposes limits on $h$, which should be at least several lattice constants or higher, because permittivity $\varepsilon_d$ trends to zero for the smaller $h$. Ferroelectric film with 180-degree domain structure and spontaneous polarization vector $\mathbf{P}_S = (0,0,\mathrm{P}_3)$ has thickness $l$. The period of 180-degree domain structure is $a$. The *ac* voltage $V_{TG}$ is applied to the top gate electrode, whereas *dc* voltage $V_{BG}$ is applied to the bottom gate electrode. The gate voltages determine the Fermi energy level $E_F$ position in graphene and hence local electron concentration. Furthermore, the driving field $E_S$ is applied across the MLG channel.

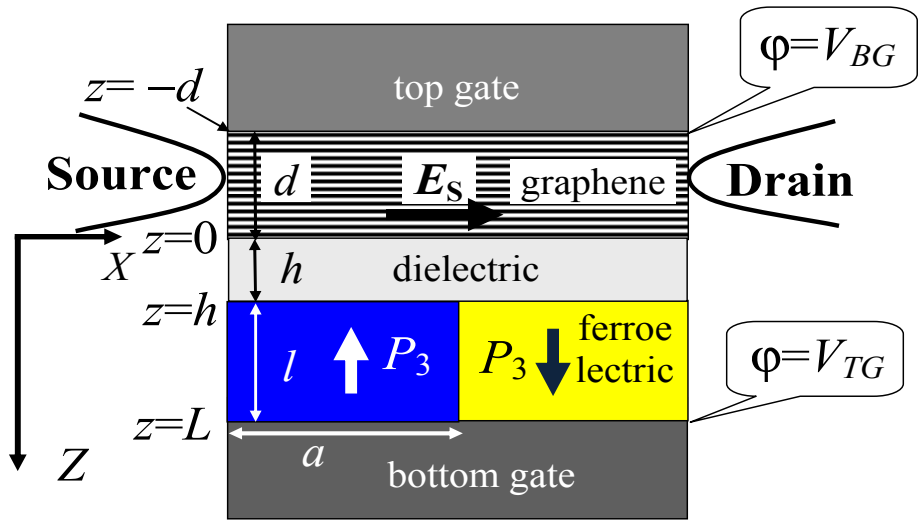


**Figure 1.** Geometry of the FET heterostructure. Shown are the top gate, MLG, dielectric layer, ferroelectric and bottom gate arranged vertically, as well as lateral source and drain electrodes.

The system of electrostatic equations for the graphene layer $(-d < z < 0)$, dielectric $(0 < z < h)$ and ferroelectric $(h < z < L)$ layers are:

$$\Delta\varphi_G - \frac{\varphi_G}{R_t^2} = 0\Big|_{-d<z<0}, \quad \Delta\varphi_d = 0\Big|_{0<z<h}, \quad \varepsilon_{33}^f \frac{\partial^2\varphi_f}{\partial z^2} + \varepsilon_{11}^f\left(\frac{\partial^2\varphi_f}{\partial x^2} + \frac{\partial^2\varphi_f}{\partial y^2}\right) = 0\Big|_{h<z<L} \quad (1)$$

Here, $\Delta$ is Laplace operator. Thickness $L = l + h$, $\varepsilon_{ij}^f$ are the linear dielectric permittivity tensor components, $R_t$ is a screening radius [22]. The latter can be estimated using Debye or Tomas-Fermi approximations depending on the electronic properties of the heterostructure.

Equations (1) are supplemented by the boundary conditions for the electric potential φ and continuity of the normal component of electric displacement **D** at the interfaces $z=-d$, $z=0$, $z=h$ and $z=L$. Displacement is related to ferroelectric polarization as $D_3^f = \varepsilon_0\varepsilon_{33}^f E_3^f + P_3$. $D_3^d = \varepsilon_0\varepsilon^d E_3^d$ in the dielectric layer and $D_3^G = \varepsilon_0\varepsilon^G E_3^G$ in the graphene ($\varepsilon_0 = 8.85\times10^{-12}$ F/m is the universal dielectric constant). When an electric current along the graphene channel is absent ($E_S = 0$), but a nonzero top and bottom gate voltages are applied, they acquire the following form:

$$\varphi_G(x,y,-d) = V_{TG}, \quad \varphi_G(x,y,0) = \varphi_d(x,y,0), \quad \varphi_d(x,y,h) = \varphi_f(x,y,h), \quad \varphi_f(x,y,L) = V_{BG} \quad (2a)$$

$$-\varepsilon_G\frac{\partial\varphi_G}{\partial z} + \varepsilon_d\frac{\partial\varphi_d}{\partial z}\Big|_{z=0} = 0, \qquad -\varepsilon_{33}^f\frac{\partial\varphi_f}{\partial z} + P_3 + \varepsilon_d\frac{\partial\varphi_d}{\partial z}\Big|_{z=h} = 0 \quad (2b)$$

In ferroelectric, the polarization is given by the time-dependent Landau-Khalatnikov (LK) equation that states

$$\Gamma\frac{\partial}{\partial t}P_3 + \alpha P_3 + \beta P_3^3 + \gamma P_3^5 - g\Delta P_3 = E_3^f, \quad (3)$$

supplemented by the natural boundary conditions, $(\partial P_3/\partial z)\big|_{z=h,L} = 0$.

### 3. Analytical solution for a single-domain state of ferroelectric

Analytical expressions for the electric potential inside each layer are listed in the **Appendix**. The electric field in ferroelectric is the sum of depolarization and external components:

$$E_3^f = E_3^d + E_3^{ext}, \quad (4a)$$

$$E_3^{ext} = \frac{\varepsilon_d\varepsilon_G\left(2V_{TG}e^{d/R_t} - V_{BG}\left(e^{2d/R_t}+1\right)\right)}{\varepsilon_d\varepsilon_G l\left(e^{2d/R_t}+1\right) + \varepsilon_{33}^f\left(\varepsilon_G h\left(e^{2d/R_t}+1\right) + \varepsilon_d R_t\left(e^{2d/R_t}-1\right)\right)}, \quad (4b)$$

$$E_3^d = \frac{-\left(\varepsilon_G h\left(e^{2d/R_t}+1\right) + \varepsilon_d R_t\left(e^{2d/R_t}-1\right)\right)\left(P_3/\varepsilon_0\right)}{\varepsilon_d\varepsilon_G l\left(e^{2d/R_t}+1\right) + \varepsilon_{33}^f\left(\varepsilon_G h\left(e^{2d/R_t}+1\right) + \varepsilon_d R_t\left(e^{2d/R_t}-1\right)\right)}. \quad (4c)$$

The field is constant in z-direction and depends on the screening radius $R_t$ and polarization $P_3$. The latter depends on $R_t$ via electric field inside the ferroelectric layer, hence yielding coupled problem.

The depolarization field leads to the film ferroelectric properties degradation with $l$ decrease and to the ferroelectricity disappearance at $l$ less than the critical value $l < l_{cr}$. The critical thickness $l_{cr}$ depends on $h$, $d$, $R_t$, dielectric permittivities $\varepsilon_G$, $\varepsilon_d$ and $\varepsilon_{33}^f$, as well as on the ferroelectric material parameter $\alpha$. At fixed $l$ value the increase of $h$ leads to a strong increase of the depolarization field and then to its value saturation, since $E_3^d \approx \frac{C_1 h + C_2}{C_3 h + C_4}$.

Since the electric field is constant in ferroelectric for the single-domain case, the solution of the LK equation of state (3) becomes consistent with the natural boundary conditions and can be obtained self-consistently from the differential (or algebraic in the stationary case) equation. The total surface charge $\sigma_G$ stored in graphene is:

$$\sigma_G = \frac{\varepsilon_0 \varepsilon_d \varepsilon_G \left(2\varepsilon_{33}^f V_{TG} e^{d/R_t} - \left(\varepsilon_{33}^f V_{BG} - \left(P_3 l/\varepsilon_0\right)\right)\left(e^{2d/R_t}+1\right)\right)}{\varepsilon_d \varepsilon_G l\left(e^{2d/R_t}+1\right) + \varepsilon_{33}^f \left(\varepsilon_G h\left(e^{2d/R_t}+1\right) + \varepsilon_d R_t\left(e^{2d/R_t}-1\right)\right)} \tag{5}$$

Note that the Eqs.(3) and (4) are coupled, and their self-consistent solution for polarization should be substituted in Eq.(5) to calculate the total charge of graphene. Then the effective surface density of carriers in graphene can be found as $n = -\left(\sigma_G / e\right)$ [3], where $e = 1.6\times10^{-19}$ C is the electron charge. Finally, the graphene "effective" electro-resistance $R$ can be estimated (see e.g. [10, 14]) as:

$$R = \frac{R_0}{\sqrt{1 + n^2/n_{res}^2}} \tag{6}$$

Here $R_0 = \frac{L_{SD}}{We\mu_{Hall} n_{res}}$, where $L_{SD}$ is a graphene's channel length from the source to the drain, $W$ is it's width, and $n_{res}$ is a residual carriers density in graphene.

### 4. Nonlinear hysteretic effect on the graphene conductivity and electro-resistance

In this section we analyze the finite size effects on the nonlinear dynamics of the space charge in a multi-layer graphene when the ferroelectric substrate is in a single-domain case. In particular we study the dependence of $P_3$, $\sigma_G$ and $R$ voltage response on ferroelectric substrate thickness $l$, dielectric layer thickness $h$ graphene thickness $d$ and screening radius $R_t$. Note that the field does not depend on MLG thickness $d$ separately, but depends on the ratio $2d/R_t$. Following the experimentally adopted configuration [8], here we assume that the bottom gate voltage is constant and the top gate voltage varies with the frequency $\omega$, i.e. $V_{TG} = V_{TG}\sin(\omega t)$. Dimensionless frequency is introduced as $w = -\omega\Gamma/\alpha$. The full set of parameters is listed in the **Table A1** in **Appendix**.

Nonlinear and hysteresis effects manifest when electric field in ferroelectric $E_3^f$ is enough to reverse or significantly change its polarization $P_3$ in agreement with Eq.(3). The polarization hysteresis immediately causes the hysteretic response of the total charge stored in multi-layer graphene and its resistance. The heterostructure response can be asymmetric, since the initial direction of polarization breaks the inversion symmetry. Generally these results correspond to the mechanism of the "direct" hysteresis in a graphene's channel resistivity, caused by the re-polarization of the substrate dipoles (see e.g. [23]).

**Figure 2** shows the ferroelectric polarization $P_3$, the effective density of the total charge stored in graphene $n$ and its electro-resistance $R$ as a function of the top gate voltages $V_{TG}$ for several values of graphene thickness $d$. At low frequencies, polarization and charge loops become very slim, strongly tilted and shifted from the coordinate origin with the thickness $d$ decrease. At higher frequencies polarization and total charge loops acquire quasi-elliptic shape with a noticeable vertical and horizontal asymmetry. Remarkably, the loops asymmetry increases with $d$ increase, while resistance loops double shape transforms into a single one for the higher values of $d$. This strong influence of the heterostructure voltage response on graphene thickness $d$ partially comes from the complex exponential dependence of the depolarization field on the parameter [curves 1-4 in **Figs 2**]..

The graphene charge loop shape, and the remnant charge and coercive voltage values strongly correlate with the polarization loop, since the charge is proportional to $P_3$ and $V_{BG}$ in accordance with Eq.(5), namely $\sigma_G = C_1 V_{TG} + C_2 V_{BG} + C_3 P_3$. Moreover, $V_{BG}$ induces non-trivial vertical and horizontal asymmetry of all the loops. The electro-resistance response is defined by the residual carrier density in the graphene, $n_{res}$, and is modulated by an order of magnitude for chosen parameters. It strongly increases with the decrease of $n_{res}$ in agreement with Eq.(6).

The resistance loop shape shown in **Figs.2f** are and very similar to the experimental ones obtained by Zheng et al (Fig.2 in [10]), while the amplitude of ac voltage applied to the top gate ($V_{TG0}$=30 V) was taken much higher than the bottom gate voltage ($V_{BG}$ =± 5 V). Note, that analytical results illustrated by **Figs.2** are complementary to the experiment and modeling performed by Zheng et al [10], because we analysed the influence of the heterostructure finite sizes on graphene sheet conductivity and resistance. Nevertheless the comparison of hysteresis loop shape observed experimentally for graphene field-effect transistors with ferroelectric gating at different back gate voltages [10] with the loop shape calculated theoretically for different thickness of multi-layer graphene demonstrates a surprising agreement (compare **Fig. 2f** with figures 2 in Ref. [10]).

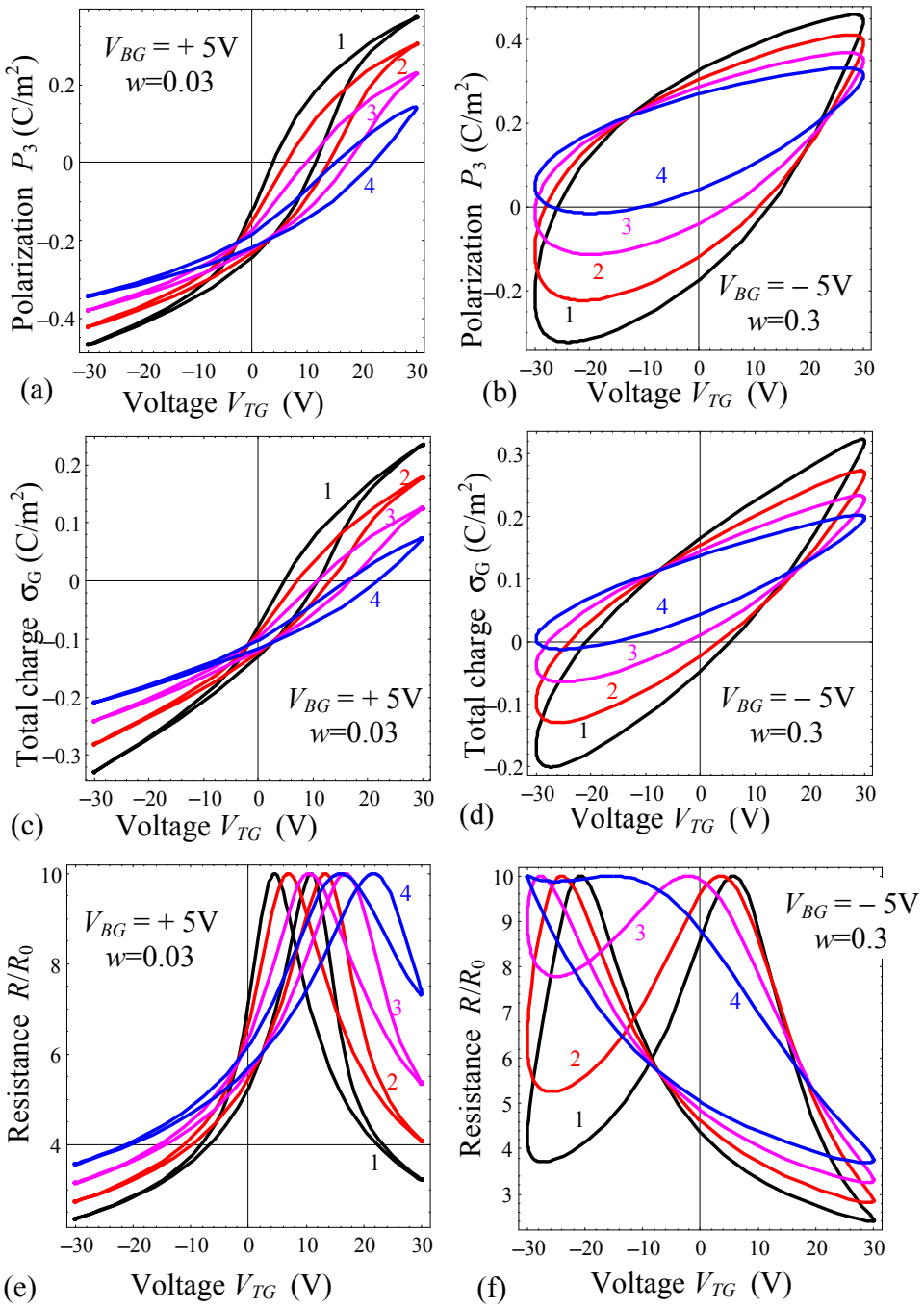


**Figure 2. Influence of multi-layer graphene thickness.** Hysteresis loops of $LiNbO_3$ ferroelectric polarization **(a, b)**, density of the total charge stored in multi-layer graphene **(c, d)** and its electro-resistance **(e, f)** calculated for different thickness of multi-layer graphene $d$=3, 4, 5, 6 nm (curves 1, 2, 3, 4). The frequency $w$=0.03 and back gate voltage $V_{BG}$= + 5 V for plots **(a)**, **(c)** and **(e)** (left column); $w$=0.3 and back gate voltage $V_{BG}$= – 5 V for plots **(b)**, **(d)** and **(f)** (right column). Sapphire dielectric thickness $h$=10 nm, screening radius $R_t$=3 nm, $n_{res}$ = 5×10$^{17}$ m$^{-2}$, ferroelectric film thickness $l$=20 nm.

**Figure 3** illustrates the dependence of the coercive voltages of graphene charge loop on the thicknesses of dielectric layer, graphene and ferroelectric film for different frequencies $w$ and positive back gate voltage $V_{BG}$. Positive and negative coercive voltages are equal for the case of $V_{BG}$=0 and different for nonzero $V_{BG}$,. The coercive voltage decreases with $h$ increase and fixed $d$ and $l$ values. At fixed $h$ the voltage almost linearly increases with $d$ increase or $l$ increase.

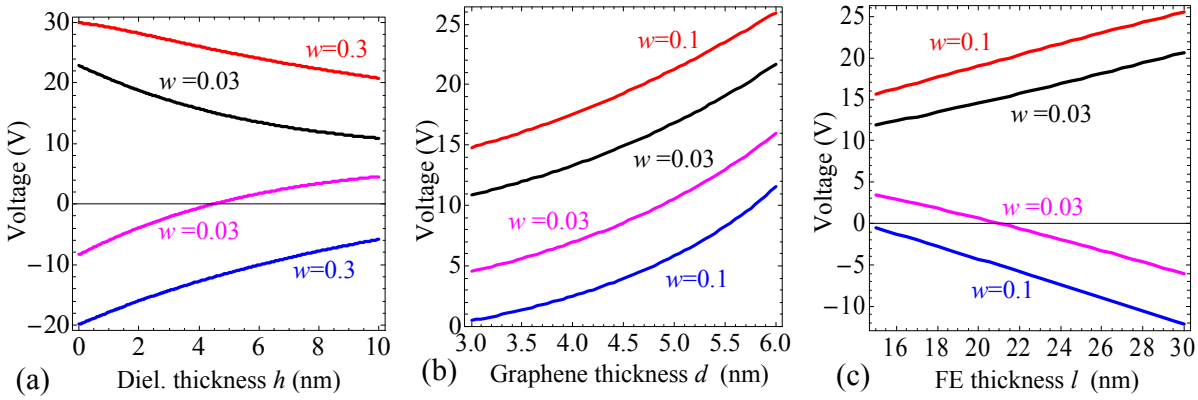


**Figure 3. Size effect of coercive voltages.** Graphene total charge left and right coercive voltages dependence on the dielectric layer, graphene and ferroelectric film thicknesses $h$, $d$ and $l$ correspondingly calculated for different frequencies $w$= 0.01 – 0.3 (labels near the curves). Plots (a), (b) and (c) are calculated with the back gate voltage 5V. For plots (a) $d$ = 3 nm, $l$ = 20 nm; (b) $h$ = 10 nm, $l$ = 20 nm; (c) $h$ = 5 nm, $d$ = 3 nm. Other parameters are the same as in the figure 2.

**Figure 4** shows the dependence of the differential electro-resistance, $\delta R = (R_{\max} - R_{\min})/R_{\min}$, on the thickness of dielectric layer, multi-layer graphene and ferroelectric film for different frequencies $w$ and fixed back gate $V_{BG}$=5 V. Dependence of $\delta R$ on $h$ has a pronounced maximum at a low frequency $w \le 0.1$. The height of maximum decreases, width increases and position shifts to the higher $h$ with $w$ increase. At fixed $h$=10 nm, the dependence of $\delta R$ on $d$ is monotonic for low frequencies $w \le 0.1$. A diffuse maxima appears at $w = 0.3$. At fixed $h$=5 nm the dependence of $\delta R$ on $l$ has a pronounced maximum at the low frequencies $w \le 0.1$. Note, that revealed maximum and its properties size dependence can be of great importance for optimization of GFeFET performances, especially for the application in nonvolatile memory devices of new generation, where large $\delta R$ is needed.

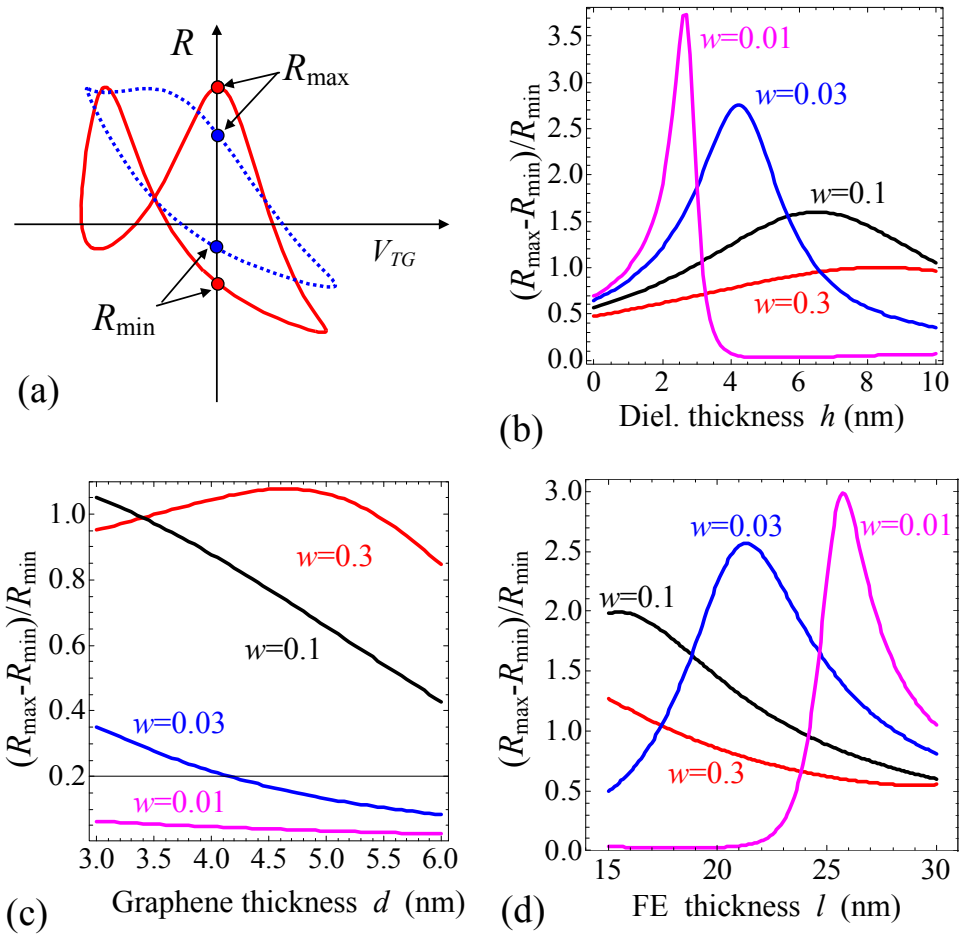


**Figure 4. Size effect on graphene electro-resistance.** **(a)** Definition of the value $\delta R = (R_{max} - R_{min})/R_{min}$ for resistance loops of different shape. **(b-d)** Dependences of $\delta R$ on the dielectric layer, graphene and ferroelectric film thicknesses $h$, $d$ and $l$ calculated for different frequencies $w$= 0.01 – 0.3 (labels near the curves) are shown in the plots **(b)**, **(c)** and **(d)** correspondingly. Back gate voltage is $V_{BG}$=5 V; top gate voltage amplitude is 30 V and. Parameters for the plot (b): $R_t$=3nm, $d$=3nm, $l$=20nm; (c) $R_t$=3nm, $h$=10nm, $l$=20nm; (d) $R_t$=3nm, $h$=5nm, $d$=3nm. Other parameters are the same as in the figure 2.

To summarize the modelling results presented in the section, first of all let us underline that the system graphene-on-ferroelectric demonstrates pronounced finite size effects. Using this fact one can effectively control and optimize the nonlinear and hysteretic properties of the system by varying the thicknesses of the layers. Secondly, our theoretical approach is capable to describe available experimental results.

### 5. Domain structure impact on the equilibrium space charge redistribution in MLG

We further consider a ferroelectric film with the domain stripes, which domain walls are perpendicular to the film surface and to the transport direction along the graphene channel (see Figure 1). The orientation of domain stripes is typical for thin ferroelectric films, especially for uniaxial ferroelectrics. External electric dragging field $E_S$ is applied in x-direction between the source and drain electrodes located at graphene surface $z=-d$. In this case, one of the boundary conditions (see Eqs.(2)) should be modified as $\varphi_G(x,y,z=-d)=V_{TG}-xE_S$. Stationary solution for electric potential in a multi-domain state of ferroelectric is listed in the **Appendix A** [24]**.** For the orientation the depolarization field induced by the stripes has maximal component directed along the dragging field $E_S$. The component is minimal (ideally absent) for the domain walls parallel to the film surface. Hence the chosen orientation of domain stripes corresponds to the maximal impact of the domain structure on the transport properties of graphene.

Below we study the space charge redistribution caused by domain stripes for the system "multi-layered graphene/dielectric/ferroelectric thin film" Full set of parameters are listed in the **Table A1.** Complex size effects possibly appeared in the case of domain stripe period $a \sim h$ will be considered elsewhere. Below we mainly use the value of 500 nm that is much higher than graphene and dielectric thickness. Applied fields $E_S = (0 - 10^3)$V/m are typical for the graphene-on-ferroelectric devices [21].

According to a well-known electrostatic problem, the electric field caused by the periodic distribution of the surface charges with alternating sings exponentially vanishes with the distance from the surface. Thus when the period of the domain stripes $a$ becomes comparable or smaller than the thickness of dielectric layer $h$, the influence of the depolarization field on the electric transport in graphene gradually decreases and practically disappears at $a<<h$. The gradual decrease of the depolarization field leads to the transformation of the rectangular-like space charge modulation in graphene to shallow harmonic modulation that vanishes in the limit $a<<h$. When the period of domain stripes becomes much larger than $h$, the depolarization field in the central part of any stripe tends to the single-domain limit given by Eq.(4c) and corresponding space charge modulation acquires pronounced rectangular-like profile.

**Figures 5a, b** illustrate the influence of applied field $E_S$ and dielectric gap thickness on the space charge density distribution in the MLG modulated by the ferroelectric domain stripes. Within Tomas-Fermi or Debye approximations, the space charge density is proportional to the electric potential, so their spatial modulations are in the antiphase. In the case of ultra-thin dielectric layer ($h$<10 nm) the potential and space charge distributions are strongly affected by the depolarization field created by domains. In this case $h$>10 nm and 0<$E_S$<50 V/m, and the charge density x-profile is quasi-

harmonic function with maxima in the centre of domains and zero values on domain wall. The effect is manifested as quasi-rectangular modulation for $E_S$=0 and have a slightly incline step for 0<$E_S$<500 V/m. The steps becomes smoother and smaller with the $h$ increase and almost disappear at the $h$=50 nm and $E_S$>50 V/m indicating that for this case the external field effect appeared stronger than the depolarization field influence near the graphene upper surface $z = -d$ . The event can be interpreted as a field-induced phase transition of the second order. Note that for $E_S$ smaller than some critical value (< 1 kV/m) there are $p$ and $n$ domains in MLG with electrons and holes conductivity correspondingly, and the dominant scattering mechanism thus can be due to the $p$-$n$-junction at the domain walls (see [25] and refs therein). For the higher fields there are no $p$ and $n$ domains, suggesting the change of the dominant scattering mechanism (e.g. towards scattering on the charged impurities, present in the dielectric layer [2] or on the interface, which is generally less intensive than the long-range disorder scattering, described in [23]) and the dramatic increase of the MLG channel conductivity. The effect can be used in ferroelectric and sensoric applications.

The total charge density calculated at $E_S$=1 kV/m is shown in the **Figures 5c-d** for $h$=5 and dielectric layer thickness $h$=50 nm. Plots illustrate the monotonic decrease of the maximal total charge with graphene thickness increase, i.e. finite size effect. Saturation appears with the $d$ increase.

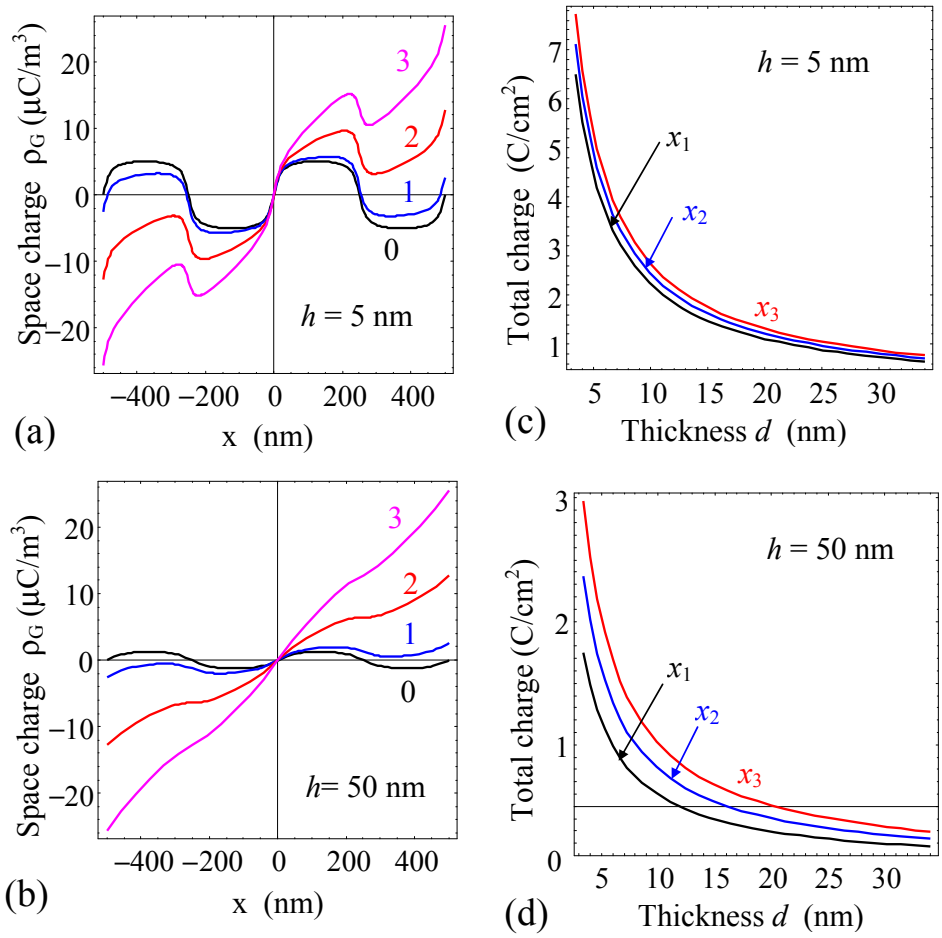


**Figure 5. Effect of domain stripes. (a, b)** Space charge x-distribution at $z = -d + R_t/2 =$ –3.15 nm caused in MLG by ferroelectric domain stripes in Roshelle salt, with the presence of sapphire layer of different thickness $h$=5 nm and 50 nm on ferroelectric surface. Driving electric field $E_S$=0, 10, 50 and 100V/m (curves with labels 0, 1, 2 and 3 correspondingly), $V_{TG}$=$V_{BG}$=0. Ferroelectric film thickness $l$=300 nm, domain stripe period $a$=500 nm, MLG thickness $d$=3.4 nm (N=10 graphene layers), multi-layered graphene permittivity $\varepsilon_G$=15 (graphite), Thomas-Fermi screening radius in graphene is $R_t$=0.5 nm. **(c-d)** Total charge dependence on MLG thickness $d$ calculated at different x-coordinates $x_1$= 125 nm, $x_2$= 725 nm and $x_3$= 1125 nm. The results are field-dependent, here we put $E_S$=1 kV/m.

Finally we expect a rather strong orientation dependence of the transport properties on the domain stripes direction with respect to the film surface. The effect can open the possibility of additional transport control in graphene by triggering the domain walls orientation in multiaxial ferroelectric substrate. Unfortunately the interesting question is beyond the scope of the present study.

## 7. Conclusion

We propose the combined self-consistent approach to describe graphene-on-ferroelectric dynamic behaviour and obtained analytical results describing finite size effect in the system, which are the first necessary step to transform the state-of-the-art from an empirical to an analytical level. Basic results obtained in this work are the following.

The main physical factor responsible for the resisting memory effect in the considered heterostructure "multi-layer graphene–dielectric layer–ferroelectric film" is the hysteresis of the internal depolarizing electric field, which appears in the dielectric layer between multi-layer graphene and ferroelectric film. The depolarizing fields originated from the incomplete screening of ferroelectric film spontaneous polarization in the dielectric layer. Since the field reverses its sign under the spontaneous polarization reversal taking place when external field exceeds the coercive one (ferroelectric hysteresis), the process causes nonlinear hysteretic dynamics of graphene charge and electro-resistance.

The analytical expressions for the acting electric field, graphene charge and electro-resistance are derived in the case when a uniformly polarized ferroelectric film is a perfect insulator, and its surface is free of screening charges. As anticipated the field value is defined by the thicknesses of dielectric layer $h$, multi-layer graphene film $d$, and ferroelectric film $l$. The analytical expressions helps us to reach a comprehensive understanding of the physical process, as well as to predict and to analyze multi-scale finite size effects in the system, which in turn opens an effective way to control and optimize its nonlinear and hysteretic properties. In particular, versatile shape of graphene charge and electro-resistance hysteresis loops appears in the system depending on the layers thicknesses $h$, $l$ and $d$, and frequency and amplitude of electric voltage applied to the top gate (see **Table 1**). Note that calculated resistance loops are very similar to the experimental ones obtained earlier by Zheng et al [10] in GFeFET and correlate with the mechanism of the “direct” hysteresis of graphene channel resistivity, caused by re-polarization of the dipoles in ferroelectric substrate [23].

The approach proposed for a single-domain film can be further evolved for the description of the space charge accumulation in the graphene-on-ferroelectric allowing for the ferroelectric domain structure. In particular, when the ferroelectric substrate has evolved stripe domain structure and a driving electric field $E_S$ is applied along the graphene channel, the domain stripes of different polarity can induce domains with $p$ and $n$ conductivity in a multi-layer graphene strip for $E_S$ smaller then some critical value. Thus for the case the dominant carrier scattering mechanism can be randomly distributed $p$-$n$-junction potentials, which position correlates with the domain walls in ferroelectric film. For the higher fields there are no pronounced $p$ and $n$ domains, only smeared ripples remained, which indicates the change of the dominant scattering mechanism and the dramatic increase of the graphene

channel conductivity. The intriguing effect can open new possibilities for graphene-based sensors and explore the physical mechanisms underlying the operation of graphene field effect transistor with ferroelectric gating.

**Table 1. Finite size effects**

<table>
<tr><th>Size</th><th>Influence on polarization $P_3$</th><th>Influence on total charge $\sigma_G$</th><th>Influence on electro-resistance $R$ and its variation $\delta R = (R_{\max} - R_{\min})/R_{\min}$</th></tr>
<tr><td rowspan="2">Dielectric layer thickness $h$</td><td>Remnant polarization decreases with increasing $h$</td><td>The total charge maximal difference (amplitude) decreases with increasing $h$.</td><td rowspan="2">Double peaks of resistance dependence get closer and become less “sharp” with $h$ increase. $\delta R(h)$ has a pronounced maximum at low frequencies, which height decreases, width increases and position shifts to higher $h$ values with frequency increase</td></tr>
<tr><td colspan="2">Coercive voltages, as well as the maximal loop width, decrease with increasing $h$. The loops lose the squire-like and acquire slim-like shape with $h$ increase.</td></tr>
<tr><td rowspan="2">Multi-layer graphene thickness $d$</td><td>Remnant polarization decreases with increasing $d$</td><td>The total charge amplitude decreases with increasing $d$</td><td rowspan="2">The loops asymmetry increases with $d$ increase and double shape loops transform into a single shape.</td></tr>
<tr><td colspan="2">Coercive voltages, as well as the maximal loop width, decrease with increasing $d$. For layers of graphite (more than 30 graphene layer) hysteresis loops are not revealed</td></tr>
<tr><td rowspan="2">Ferroelectric thickness $l$</td><td>Remnant polarization values decrease with $l$ decrease.</td><td>The total charge amplitude decreases with decreasing $l$.</td><td rowspan="2">The difference between two peaks of resistance increases with increasing $l$. $\delta R(l)$ has a maximum at low frequencies, which height decreases, width increases and position shifts to smaller $l$ values with frequency increase</td></tr>
<tr><td colspan="2">Coercive voltage values decrease with $l$ decrease.</td></tr>
<tr><td rowspan="2">Screening radius $R_t$</td><td>Remnant polarization decreases with increasing $R_t$.</td><td>Total charge value becomes smaller with $R_t$ increase.</td><td>Resistance loops double shape transforms into a single one with $R_t$ increase.</td></tr>
<tr><td colspan="3">Coercive voltage values decreases with increasing $R_t$, hysteresis loop almost disappears when multi-layer graphene thickness $d$ becomes more than $2R_t$. Loops become smoother with increasing $R_t$.</td></tr>
</table>

**Acknowledgments.** A.N.M., O.V.V. and E.A.E. acknowledge National Academy of Sciences of Ukraine, grant 35-02-14, and Center for Nanophase Materials Sciences, user projects CNMS 2013-293, CNMS 2014-270. Research for SVK was supported by the US Department of Energy, Basic Energy Sciences, Materials Sciences and Engineering Division. The authors are very grateful to Lisa A. Goins for helping with the manuscript preparation.

## Appendix

The contribution of the top and bottom gate potentials $V_{TG}$ and $V_{BG}$ and polarization $P_3$ into the solution of the boundary problem (1)-(3) are given by these expressions:

$$\varphi_G(z)=\frac{\begin{pmatrix}V_{TG}\left(e^{(d+z)/R_t}\varepsilon_d\varepsilon_G l\left(e^{-2z/R_t}+1\right)+\varepsilon_{33}^f\left(\varepsilon_G h\left(e^{-2z/R_t}+1\right)+\varepsilon_d R_t\left(e^{-2z/R_t}-1\right)\right)\right)\\+\varepsilon_d R_t\left(\varepsilon_{33}^f V_{BG}-\left(P_3 l/\varepsilon_0\right)\right)\left(e^{(2d+z)/R_t}-e^{-z/R_t}\right)\end{pmatrix}}{\varepsilon_d\varepsilon_G l\left(e^{2d/R_t}+1\right)+\varepsilon_{33}^f\left(\varepsilon_G h\left(e^{2d/R_t}+1\right)+\varepsilon_d R_t\left(e^{2d/R_t}-1\right)\right)}, \quad \text{(A.1a)}$$

$$\varphi_d(z)=\frac{2V_{TG}e^{d/R_t}\left(\varepsilon_d l+\varepsilon_{33}^f(h-z)\right)\varepsilon_G+\left(\varepsilon_{33}^f V_{BG}-\left(P_3 l/\varepsilon_0\right)\right)\left(\varepsilon_d R_t\left(e^{2d/R_t}-1\right)+\varepsilon_G z\left(e^{2d/R_t}+1\right)\right)}{\varepsilon_d\varepsilon_G l\left(e^{2d/R_t}+1\right)+\varepsilon_{33}^f\left(\varepsilon_G h\left(e^{2d/R_t}+1\right)+\varepsilon_d R_t\left(e^{2d/R_t}-1\right)\right)}, \quad \text{(A.1b)}$$

$$\varphi_f(z)=V_{BG}+(h+l-z)\frac{\varepsilon_d\varepsilon_G\left(2V_{TG}e^{d/R_t}-V_{BG}\left(e^{2d/R_t}+1\right)\right)-\left(\varepsilon_G h\left(e^{2d/R_t}+1\right)+\varepsilon_d R_t\left(e^{2d/R_t}-1\right)\right)\left(P_3/\varepsilon_0\right)}{\varepsilon_d\varepsilon_G l\left(e^{2d/R_t}+1\right)+\varepsilon_{33}^f\left(\varepsilon_G h\left(e^{2d/R_t}+1\right)+\varepsilon_d R_t\left(e^{2d/R_t}-1\right)\right)} \quad \text{(A.1c)}$$

where the subscript $j=G,d,f$ means graphene, dielectric and ferroelectric correspondingly.

Using a screening radius approximation Eq.(1) (see also [4]) the space charge density $\rho_G(z)$ in the multi-layered graphene is given by the expression $\rho_G(z)=-\varepsilon_0\varepsilon_G\frac{\varphi_G(z)}{R_t^2}$. The total charge $\sigma_G$ is the sum of the integrated over graphene thickness space charge density $\rho_G(z)$ and the surface charge are determined by the boundary condition at the graphene-top gate interface $z=-d$ as $D_3^G(-d)=\sigma_S$. In accordance with the principle of the whole system electro neutrality, the total charge stored in graphene is opposite in sign to the electric displacement at the bottom electrode, $D_3^f\big|_{z=L}=\left(\varepsilon_0\varepsilon_{33}^f E_3^f+P_3\right)\big|_{z=L}$, that in allowance for Eq.(4) gives Eqs.(5).

**Table A1. Range of parameters used in calculations**

| **Parameters** | **Value** |
|---|---|
| screening radius $R_t$ | (0.3 - 3) nm |
| graphite permittivity $\varepsilon_G$ | 15 |
| graphene thickness $d$ | (3 – 30) nm |
| residual concentration $n_{res}$ | (vary from $10^{17}$ $m^{-2}$ to $10^{15}$ $m^{-2}$, as the latter value was used in [10]) |
| dielectric permittivity $\varepsilon_d$ | 1(air); 5-7 (background constant), 12.53 (sapphire $Al_2O_3$) |
| dielectric layer thickness $h$ | (0 – 50) nm |
| dielectric anisotropy of ferroelectric $\gamma$ | 0.58 ($LiNbO_3$); 3.87 (Rochelle salt) |
| ferroelectric permittivity $\varepsilon_{33}^f$ | 29 ($LiNbO_3$); 300 (Rochelle salt) |
| ferroelectric polarization $P_S$ | 0.75 C/$m^2$ ($LiNbO_3$); 0.002 C/$m^2$ (Rochelle salt or relaxor) |
| LGD parameters for $LiNbO_3$ | $\alpha=-1.95\times10^9$ m/F, $\beta=3.61\times10^9$ $m^5/(C^2F)$, $\gamma=0$ |
| ferroelectric thickness $l$ | (10 – 30) nm |
| period of domain structure $a$ | (50 – 500) nm |
| coercive field range | $(2-7)\times10^8$ V/m ($LiNbO_3$); 30 kV/cm (Rochelle salt) |

## References


[1] Novoselov K. S. *et al.* «Two-dimensional gas of massless Dirac fermions in graphene», Nature **438**, 197 (2005) DOI:10.1038/nature04233

[2] A.Geim. Science, **324**, 1530 (2009)

[3] K. Novoselov, A. Geim, S. Morozov, *D.* Jiang, Y. Zhang, S. Dubonos, I. Grigorieva, A. Firsov, Science, **306**, 666 (2004)

[4] S. Das Sarma, Shaffique Adam, E.H. Hwang, E.Rossi, Rev. Mod. Phys. **83**, 407 (2011)

[5] N.M.R. Peres, Rev. Mod. Phys. **82**, 2673 (2010)

[6] S. Kim, J. Nah, I. Jo, D. Shahrjerdi, L. Colombo, Z. Yao, E. Tutuc, S. K. Banerjee, Appl. Phys. Lett. **94**, 062107 (2009)

[7] A. Konar, T. Fang, D. Jena. Phys. Rev. **B. 82**, 115452 (2010).

[8] Yi Zheng, Guang-Xin Ni, Chee-Tat Toh, Ming-Gang Zeng, Shu-Ting Chen, Kui Yao, Barbaros Özyilmaz, Appl. Phys. Lett. **94**, 163505 (2009).

[9] X. Hong, J. Hoffman, A. Posadas, K. Zou, C. H. Ahn, J. Zhu. Appl. Phys. Lett. **97**, 033114 (2010).

[10] Yi Zheng, Guang-Xin Ni, Chee-Tat Toh, Chin-Yaw Tan, Kui Yao, Barbaros Özyilmaz. Phys. Rev. Lett. **105**, 166602 (2010).

[11] Yi Zheng, Guang-Xin Ni, Sukang Bae, Chun-Xiao Cong, Orhan Kahya, Chee-Tat Toh, Hye Ri, Kim, Danho Im, Ting Yu, Jong Hyun Ahn, Byung Hee Hong, Barbaros Özyilmaz. Europ. Phys. Lett. **93**, 17002 (2011).

[12] Emil B. Song, Bob Lian, Sung Min Kim, Sejoon Lee, Tien-Kan Chung, Minsheng Wang, Caifu Zeng, Guangyu Xu, Kin Wong, Yi Zhou, Haider I. Rasool, David H. Seo, Hyun-Jong Chung, Jinseong Heo, Sunae Seo, Kang L. Wang, Appl. Phys. Lett. **99**, 042109 (2011).

[13] Guang-Xin Ni, Yi Zheng, Sukang Bae, Chin YawTan, Orhan Kahya, Jing Wu, Byung Hee Hong, Kui Yao, Barbaros Özyilmaz. ACSNano **6**, 3935 (2012).

[14] Santosh Raghavan, I. Stolichnov, N. Setter, J.-S. Heron, M. Tosun, A. Kis, Appl. Phys. Lett. **100**, 023507 (2012)

[15] M. Humed Yusuf, B. Nielsen, M. Dawber, X. Du., Nano Lett, **14** (9), 5437 (2014)

[16] A. N. Morozovska, M. V. Strikha. J. Appl. Phys. **114**, 014101 (2013)

[17] A. N. Morozovska, E. A. Eliseev, A. V. Ievlev, O. V. Varenyk, A. S. Pusenkova, Ying-Hao Chu, V. Ya. Shur, M. V. Strikha, S. V. Kalinin, Journal of Applied Physics, **116**, 066817 (2014)

[18] M. V. Strikha, J. Phys. Optics. **12**, 162 (2011)

[19] X. Hong, K. Zou, A. M. DaSilva, C. H. Ahn, J. Zhu. Integrating functional oxides with graphene. Solid State Commun. **152**, 1365 (2012)

[20] M. V. Strikha, Ukr. J. Phys. Opt. **13**, S5 (2012)

[21] M.V. Strikha. Non-volatile Memory of New Generation and Ultrafast IR Modulators Based on Graphene on Ferroelectric Substrate. 163-179, Chapter in "Functional Nanomaterials and Devices for Electronics, Sensors and Energy Harvesting", ISBN 978-3-319-08803-7, DOI 10.1007/978-3-319-08804-4, Springer International Publishing Switzerland (2014)

[22] N. W. Ashcroft, N. D. Mermin, Solid State Physics (Thomson Learning, Toronto, 1976).

[23] A. I. Kurchak, A. N.Morozovska, M.V. Strikha, Ukr. J. Phys. **58**, N 5, p.472-479 (2013)

[24] Supplementary Materials to "Finite size effects of hysteretic dynamics in multi-layer graphene on ferroelectric"

[25] A. I. Kurchak, M.V. Strikha, Ukr. J. Phys. **59**, 622 (2014).